Energy Conversion and Management 100 (2015) 157–167

Contents lists available at ScienceDirect

Energy Conversion and Management

journal homepage: www.elsevier.com/locate/enconman

The optimal configuration of photovoltaic module arrays based on adaptive switching controls

Kuei-Hsiang Chao *, Pei-Lun Lai, Bo-Jyun Liao

Department of Electrical Engineering, National Chin-Yi University of Technology, No. 57, Sec. 2, Zhongshan Rd., Taiping Dist., Taichung 41170, Taiwan

ARTICLE INFO

Article history:
Received 5 June 2014
Accepted 28 April 2015
Available online 16 May 2015

Keywords:
Optimal configuration
Photovoltaic module arrays
Particle swarm optimization
Maximum power point tracker
Shading or malfunctions

ABSTRACT

This study proposes a strategy for determining the optimal configuration of photovoltaic (PV) module arrays in shading or malfunction conditions. This strategy was based on particle swarm optimization (PSO). If shading or malfunctions of the photovoltaic module array occur, the module array immediately undergoes adaptive reconfiguration to increase the power output of the PV power generation system. First, the maximal power generated at various irradiation levels and temperatures was recorded during normal array operation. Subsequently, the irradiation level and module temperature, regardless of operating conditions, were used to recall the maximal power previously recorded. This previous maximum was compared with the maximal power value obtained using the maximum power point tracker to assess whether the PV module array was experiencing shading or malfunctions. After determining that the array was experiencing shading or malfunctions, PSO was used to identify the optimal module array connection scheme in abnormal conditions, and connection switches were used to implement optimal array reconfiguration. Finally, experiments were conducted to assess the strategy for identifying the optimal reconfiguration of a PV module array in the event of shading or malfunctions.

1. Introduction

Among the many renewable energy sources, photovoltaic (PV) power generation systems produce the lowest amount of pollutants. To increase the power generation efficiency, PV systems must be located in open spaces without shade. However, shading inevitably occurs. Because PV systems are located outdoors for long durations, they are subject to the forces of nature, such as typhoons or lightning, which may lead to the deterioration and eventual malfunction of PV modules. When shading or malfunctions occur, the power output of the system declines significantly [1–4]. Therefore, resolving problems caused by shadows or malfunctions is paramount for increasing the efficiency of PV power generation systems.

Some studies of the behavior of PV arrays with different configuration of their bypass diodes [5,6] have been carried out to prove that different configuration of bypass diodes can reduce the power loss of PV arrays due to the shadowing of their PV modules. Among them, in the PV module array with no-overlapped bypass diodes, the power losses are only produced by the power consumption of the diodes, but it would be noticeable if there were too many bypass diodes and shadowed PV modules. In addition, it still generates multiple peaks in the power–voltage (P–V) characteristic curve. Therefore, an inverter connected to the PV module array cannot always achieve the maximum power point (MPP) because of its voltage range of work and the MPPT algorithm.

When PV modules experience shading or malfunctions, the affected module cannot operate normally. This alters the current–voltage (I–V) characteristic curve of the module array, and generates multiple peaks in the power–voltage (P–V) characteristic curve. The proposed solutions to this issue [7–15] involve using maximum power point tracking (MPPT) techniques that do not track local maxima if characteristic curves exhibit multiple peaks, and instead track the true maximum in standard test conditions (STC) to reduce the effects that shading or malfunctions exert on module arrays. Although these methods can increase the system power output, extremely severe shading or malfunctions can still reduce the overall power output because the connection scheme of the module array is fixed. This limits the extent of improvement provided by MPP trackers.

Another solution involves dividing a PV module array into two parts: a fixed end and an adaptive bank [16], as shown in Fig. 1. When the modules in the fixed end are partially shaded, these modules can be connected to those in the adaptive bank using an array switch. This reduces the effect that shading exerts on the

* Corresponding author. Tel.: +886 4 2392 4505x7272; fax: +886 4 2392 2156.
E-mail address: chaokh@ncut.edu.tw (K.-H. Chao).

http://dx.doi.org/10.1016/j.enconman.2015.04.080
0196-8904/

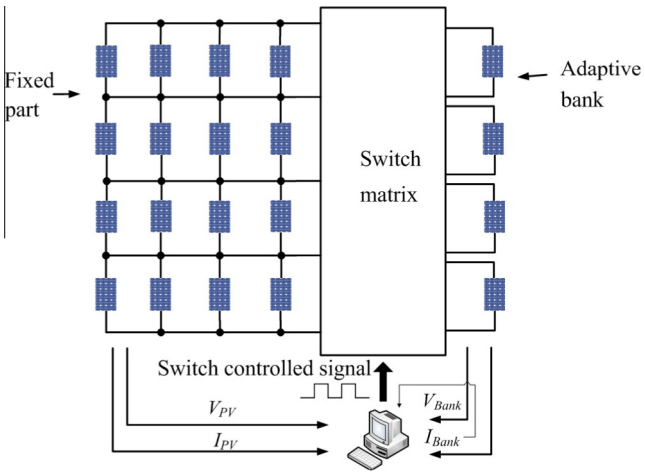

Fig. 1. Architecture of the adaptive bank presented in [16].

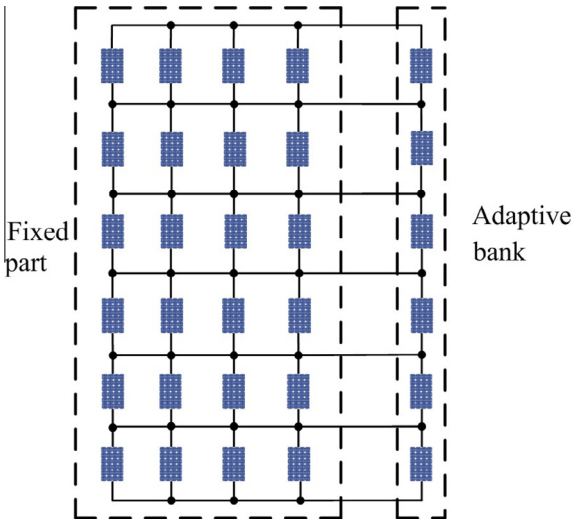

Fig. 2. Connection scheme of the module array in normal conditions presented in [16].

overall power generation system by altering the characteristics of the module connections. The module connection schemes under normal and shaded conditions are shown in Figs. 2 and 3, respectively. Although this method can effectively increase the overall power output of the system, numerous voltage and current sensors and connection switches must be configured to connect the adaptive bank to the fixed end. Substantial increases in the power output require a greater number of PV modules to be installed in the adaptive bank, which poses a substantial financial burden. Other experts and scholars have suggested using multiple MPP trackers rather than a single MPP tracker in module arrays [17] to minimize the effect that partially shaded or malfunctioning modules have on the overall system power output. This architecture is shown in Fig. 4. Although this method effectively increases the overall power output, the number of DC–DC converters required also increases equipment costs. Finally, previous research has suggested excluding shaded modules from arrays by using connection switches [18] to avoid affecting normally functioning PV modules and thus reducing the overall system performance. Figs. 5 and 6 show the connection schemes of the proposed architecture in normal and partially shaded conditions. Although this method can increase the overall power output, the connection between modules is

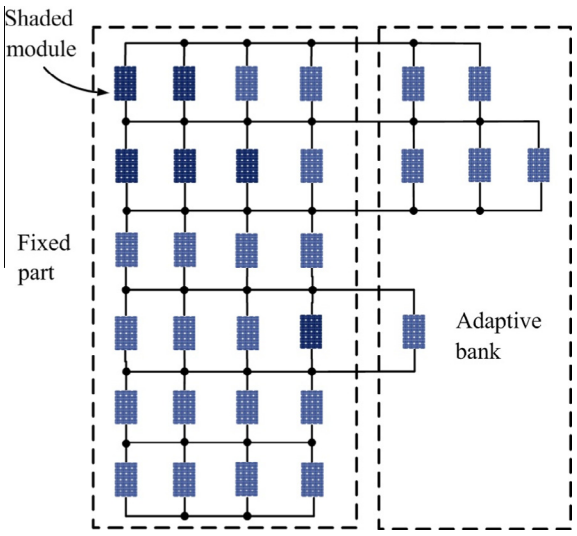

Fig. 3. Connection scheme in partially shaded conditions in [16].

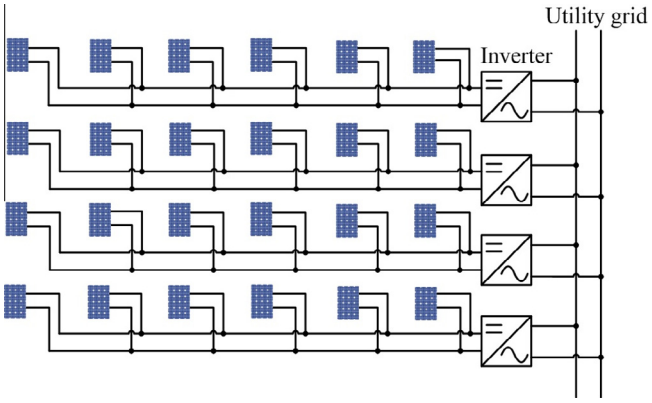

Fig. 4. Connection scheme of module arrays in [17].

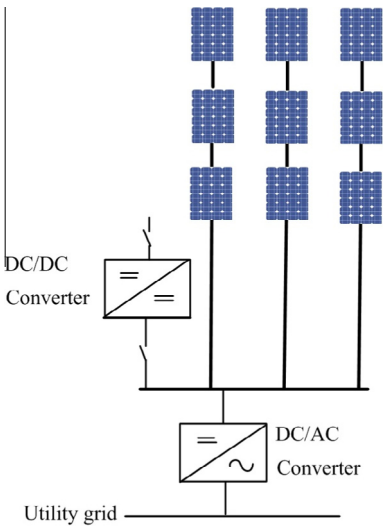

Fig. 5. Connection scheme of modules in normal conditions in [18].

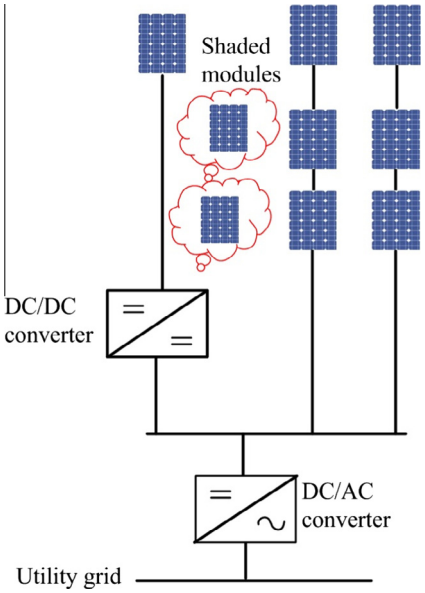

Fig. 6. Connection scheme of modules in partially shaded conditions in [18].

relatively complex, and a higher number of connection switches are required.

Accordingly, a new connection scheme for PV module arrays is proposed in this study. This configuration features only one MPP tracker and does not require a high number of connection switches. When a PV module array experiences partial shading or malfunctions, an optimization algorithm can be used to enable or disable connection switches to reconfigure the connection scheme, thereby increasing the power output of the system.

2. The power–voltage and current–voltage output characteristics of PV module arrays in normal and abnormal conditions

The *I*–V and *P*–*V* characteristic curves of PV module arrays differ in normal and abnormal conditions. Fig. 7(a) and (b) shows the *P*–*V* characteristic curves during various shading and malfunction conditions for an array of Sanyo HIP-2717 modules [19], specifically, four in series and one in parallel, with 1000 W/m^2 irradiation and a PV module surface temperature of 25 °C. Fig. 7(a) shows that if partial shading occurs on a PV module array, the *P*–*V* characteristic curve exhibits multiple peaks. However, when partial malfunction occurs, although the *P*–*V* characteristic curve does not exhibit multiple peaks, the power output decreases significantly.

3. PV module array architectures

Configurations of PV module arrays are widely investigated by contemporary experts and scholars. The following six module configurations are commonly observed [20,21]:

(1) *Series Array:* All PV modules are serially connected, as shown in Fig. 8(a). Although a serial configuration can increase the voltage output of the array, if modules experience partial shading or malfunctions, the overall voltage output declines substantially.
(2) *Parallel Array:* All PV modules are connected in parallel, as shown in Fig. 8(b). Although a parallel configuration can increase the current output of the array, if modules experience partial shading or malfunctions, the overall current output decreases.

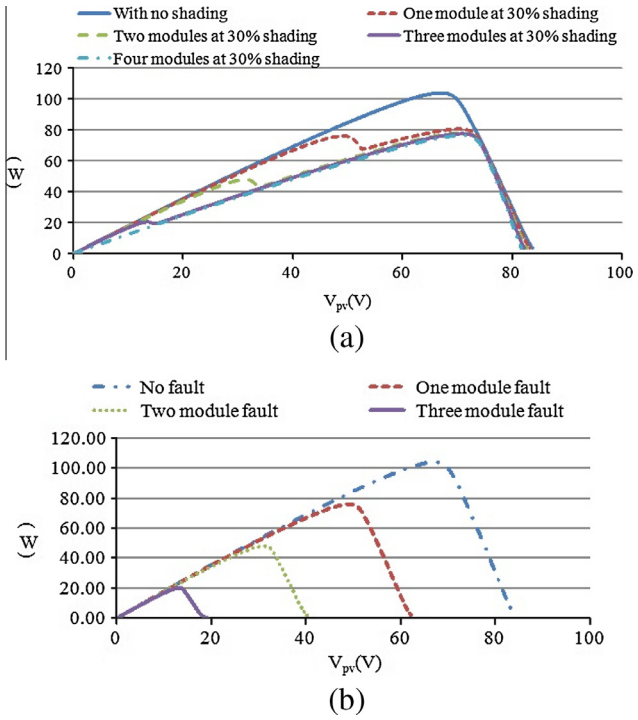

Fig. 7. The *P*–*V* characteristic curves of a Sanyo HIP-2717 array (four in series and one in parallel), with PV module surface temperature of 25 °C and irradiation of 1000 W/m^2: (a) when the modules are 30% shaded; and (b) when malfunctions occur.

(3) *Series-Parallel (SP) Array:* All PV modules are first connected serially then in parallel, as shown in Fig. 8(c). This type of configuration can increase the voltage and current output of the module array, and the connection scheme is simple and easy to construct. Consequently, series-parallel arrays are the most commonly employed configurations. However, when any branch of a series-parallel array experiences partial shading or malfunctions, the overall current output declines substantially.
(4) *Total Cross-Tied (TCT) Array:* All PV modules are connected serially and then cross-tied in parallel, as shown in Fig. 8(d). This configuration involves a scheme in which the modules are connected in parallel and then in series. Multiple PV modules are first connected in parallel; these parallel modules are then connected in series. This connection scheme can resolve the disadvantages of series and parallel arrays.
(5) *Bridge-Linked (BL) Array:* All PV modules are connected using a bridge architecture, as shown in Fig. 8(e). When configurations of this type are partially shaded, the neighboring modules are also affected, reducing the overall voltage and current output. The MPPT method proposed in [7] cannot be applied to this connection scheme.
(6) *Honeycomb (HC) Array:* All PV modules are connected in a honeycomb-like architecture, as shown in Fig. 8(f). Such configurations can reduce power output losses in some, but not all, shading conditions. Therefore, this connection scheme possesses insufficient robustness.

The voltage, current, and power outputs of the six PV module connection schemes are summarized in Table 1.

The power outputs of the six configurations mentioned previously are approximately equal at identical irradiation levels and temperatures when no shading or malfunctions occur. However, when shading or malfunctions occur, the power outputs of the

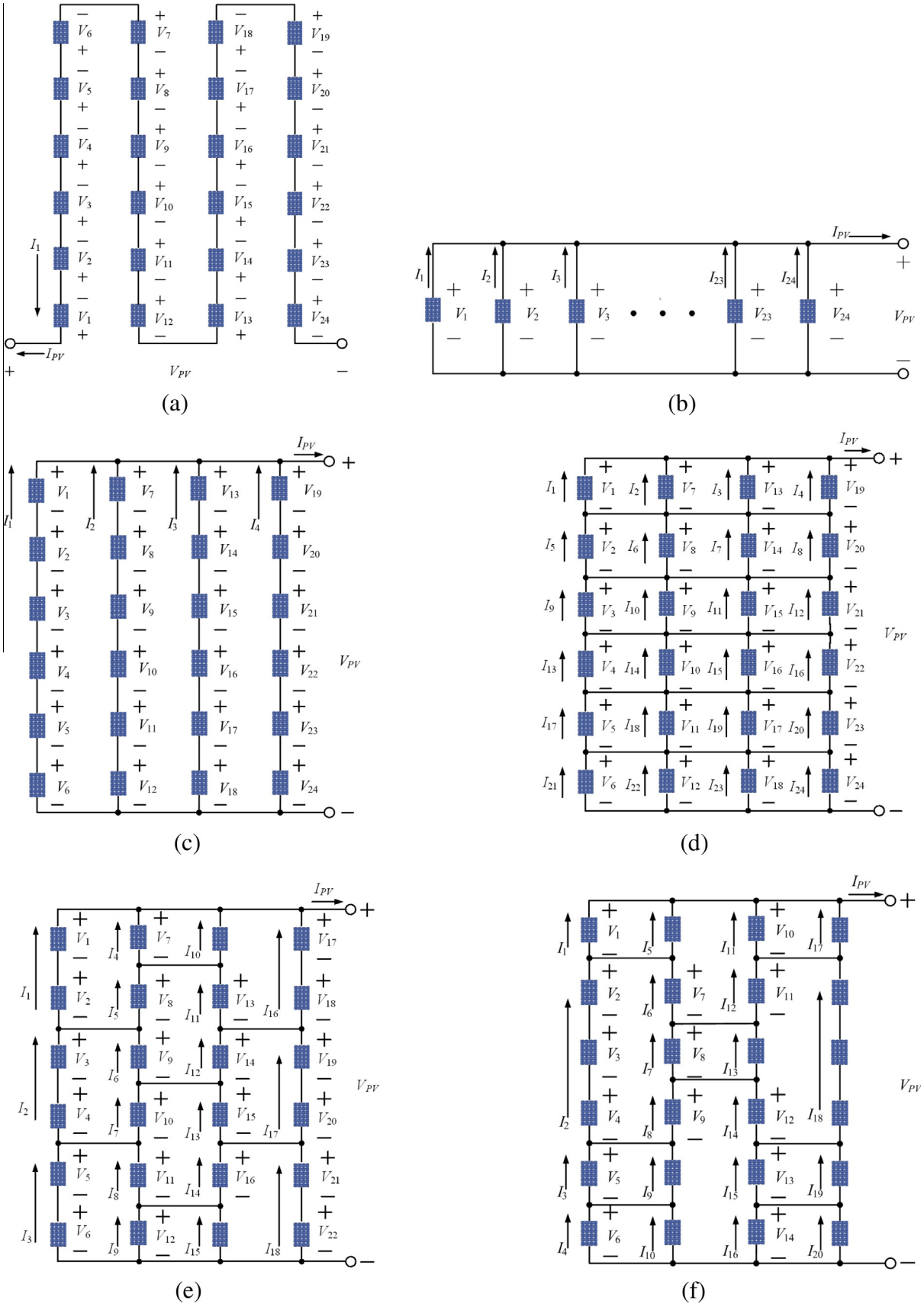

Fig. 8. Configurations of PV module arrays: (a) serial connection scheme; (b) parallel connection scheme; (c) series-parallel connection scheme; (d) total cross-tied connection scheme; (e) bridge-linked connection scheme; and (f) honeycomb connection scheme.

Table 1
The voltage, current, and power outputs of all PV module connection schemes.

Configuration	Output		
	Output voltage of array	Output current of array	Output power of array
Series array	$V_{PV}=\sum_{k=1}^{k=24}V_k=24V^*$	$I_{PV}=I_1=I^{**}$	$P_{PV}=24VI$
Parallel array	$V_{PV}=V_1=V$	$I_{PV}=\sum_{n=1}^{n=24}I_n=24I$	$P_{PV}=24VI$
SP array	$V_{PV}=\sum_{k=1}^{k=6}V_k=6V$	$I_{PV}=\sum_{n=1}^{n=4}I_n=4I$	$P_{PV}=24VI$
TCT array	$V_{PV}=\sum_{k=1}^{k=6}V_k=6V$	$I_{PV}=\sum_{n=1}^{n=4}I_n=4I$	$P_{PV}=24VI$
BL array	$V_{PV}=\sum_{k=1}^{k=6}V_k=6V$	$I_{PV}=I_1+I_4+I_{10}+I_{16}=4I$	$P_{PV}=24VI$
HC array	$V_{PV}=\sum_{k=1}^{k=6}V_k=6V$	$I_{PV}=I_1+I_5+I_{11}+I_{17}=4I$	$P_{PV}=24VI$

Notes: V^* is the voltage output of a single module.
I^{**} is the current output of a single module.

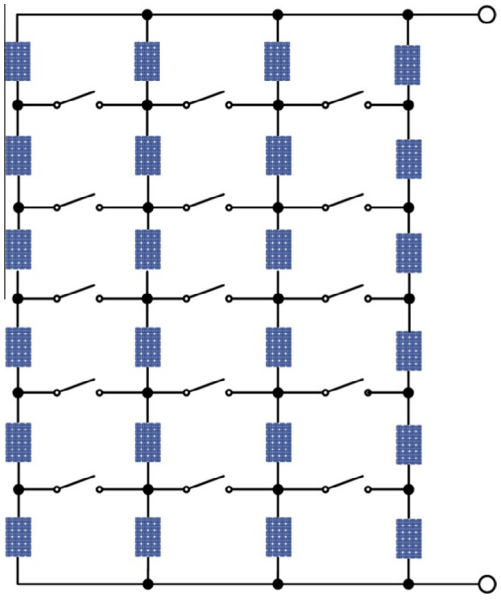

Fig. 9. The proposed connection scheme for a PV module array.

configurations differ primarily because of differences in the connection schemes. When a PV module is shaded, its voltage and current outputs are reduced, which further lowers the voltage and current outputs of neighboring series- or parallel-connected PV modules, thereby inducing a decline in the overall power output. Accordingly, this study proposes a strategy for optimizing the configuration of module arrays when shading or malfunctions occur to improve the power output of PV module arrays even in shaded or malfunction conditions.

Fig. 9 shows the connection scheme of the optimal configuration for PV module arrays. Connection switches were installed between all branches. An optimization algorithm was employed when shading or malfunctions occurred to control the activation of switches that connect or disconnect branches to increase the power output of the entire system. The algorithm used to determine the optimal configuration was based on particle swarm optimization (PSO), which is thoroughly explained in the following section.

4. Particle swarm optimization

PSO was developed in 1995 by Kennedy and Eberhart [22,23], and is a swarm intelligence technique and a branch of evolutionary algorithms. PSO was inspired by observing the group foraging behavior of birds and is used to solve search and optimization problems [24]. The method involves envisioning a bird, known as a particle, flying in a space. The movement of each particle in the search space possesses a corresponding fitness value, and each particle is aware of its current optimal fitness value and optimal position, which is known as the personal best (p_{best}). This information represents the experience of each particle. Each particle also knows the optimal value and position of the entire swarm, which is known as the global best (g_{best}). During each iteration, the velocity and position of each particle is updated and adjusted according to the experiences of both the individual and the swarm. At the start, when particles are randomly dispersed throughout the space, if any particle is near the optimal target value in a particular region, all particles in that region swarm toward that value to search for the optimal solution. However, the optimal value for that region may only be a local optimal solution. Therefore, the search results of all particle swarms must be employed to adjust the position of the global best, thereby ensuring that all particles contribute to the swarm effect, and the global best is gradually approached [25].

The preceding explanation indicates that PSO involves distributed searches and memory, and is suitable for searches in continuous domains. Two studies have shown that fluctuations in the velocity of each particle are based on the particle velocity and distance from the individual optimal solution, as well as the distance from the global optimal solution. New velocities are used to adjust the position of the particle and update the search distance and direction of all other particles. A flowchart of the PSO algorithm is shown in Fig. 10, and the steps are described below [26].

Step 1. Establish the objective function to be optimized.
Step 2. Initialize and randomly generate a new position and velocity for each particle in the swarm.
Step 3. Using the established objective function, calculate the fitness value of each particle. Compare the fitness value of all particles to identify the personal best p_{best}. Use p_{best} to adjust the search direction of each particle.
Step 4. Compare p_{best} to the global best, g_{best}. If p_{best} is superior to g_{best}, correct g_{best}, and use the new g_{best} to adjust the individual search velocity of all particles.
Step 5. Update the velocity and position of each particle by using the PSO kernel equation:

$$v_j^{k+1}=w\times v_j^k+C_1\times rand(\cdot)\times(p_{best\,j}^k-X_j^k)+C_2\times rand(\cdot)\times(g_{best}-X_j^k) \quad (1)$$

$$X_j^{k+1}=X_j^k+v_j^{k+1} \quad (2)$$

where v_j^{k+1} and v_j^k are the velocities of particle j at times $k+1$ and k, C_1 and C_2 are learning factors, w is the inertial weight, $p_{best\,j}^k$ is the personal best for particle j at time k, g_{best} is the global best, X_j^{k+1} and X_j^k are the positions of particle j at times $k+1$ and k, and $rand(\cdot)$ is a random real number between 0 and 1.
Step 6. Repeat calculations of the fitness value based on the objective function until the global optimal solution is achieved or the greatest iteration number is reached.

5. The proposed controls for optimal configurations of PV module arrays

5.1. The proposed connection scheme for PV module arrays

Fig. 11 is a diagram of the system architecture for optimal configurations of PV module arrays. The primary subsystems were a boost converter, MPPT controller, and optimal configuration controller. The MPPT controller was used to control the boost

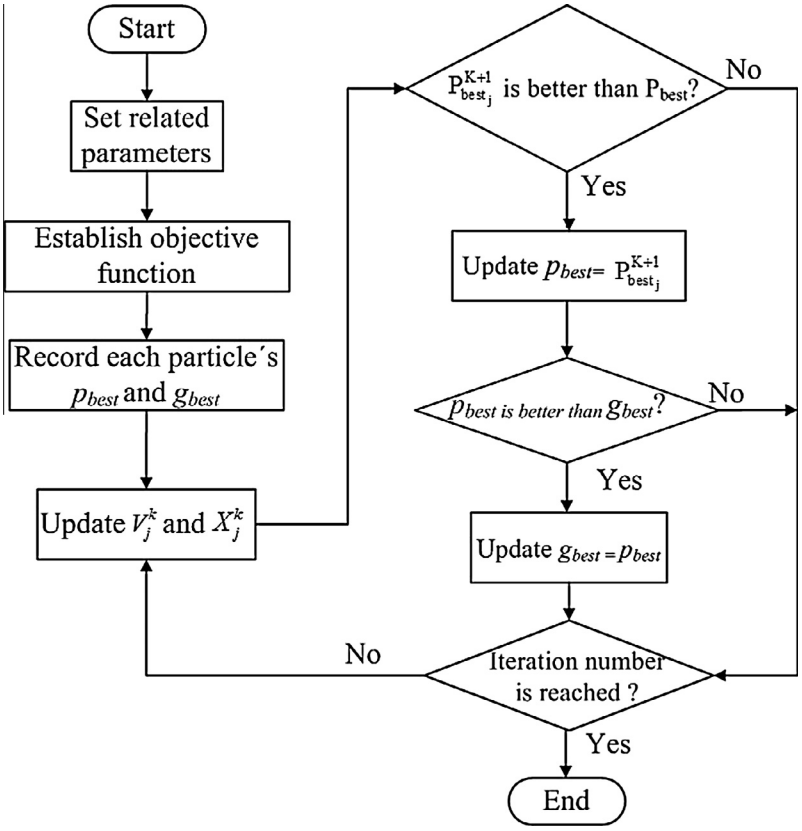

Fig. 10. A flowchart of the PSO algorithm.

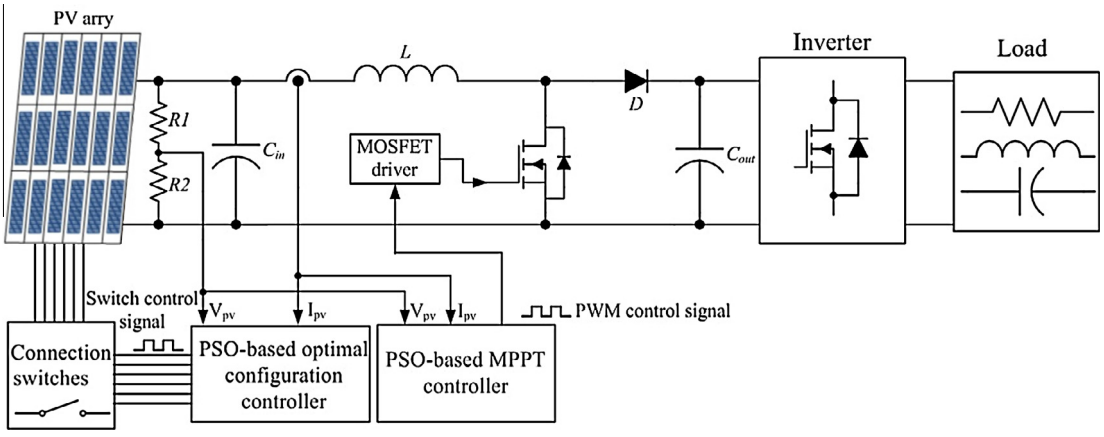

Fig. 11. A diagram of the system architecture for optimal configurations of PV module arrays.

converter to ensure that the PV module array can achieve the maximum power transfer. Under normal conditions, the optimal configuration controller is inactive and maintains the original connection scheme of the PV module array. However, when shading or malfunctions occur, the optimal configuration controller detects the voltage and current output of the module array and calculates the optimal power. The controller then determines the connection scheme capable of generating the optimal power output in the specific shading or malfunction conditions. Subsequently, the

Table 2
Electrical parameter specifications for Sanyo HIP-2717 modules.

Maximum output power (P_{max})	27.87 W	Short-circuit current (I_{sc})	1.82 A
Maximum power point current (I_{mpp})	1.63 A	Open-circuit voltage (V_{oc})	21.6 V
Maximum power point voltage (V_{mpp})	17.1 V		

Table 3
PSO parameters.

Particle number	4	Inertia weight (w)	0.8
Learning factor (C_1)	1	Interaction	8
Learning factor (C_2)	2		

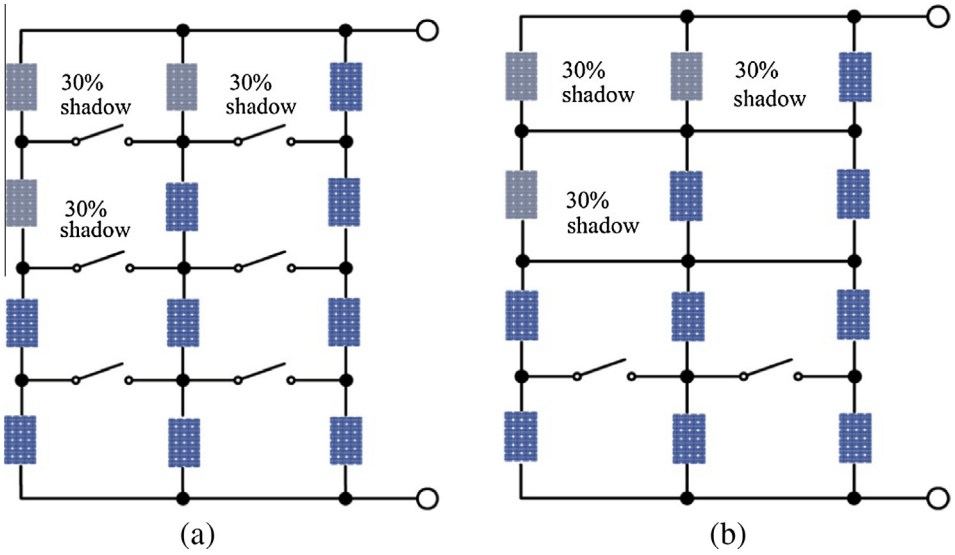

Fig. 12. Scenario 1: The connection scheme: (a) before; and (b) after reconfiguration.

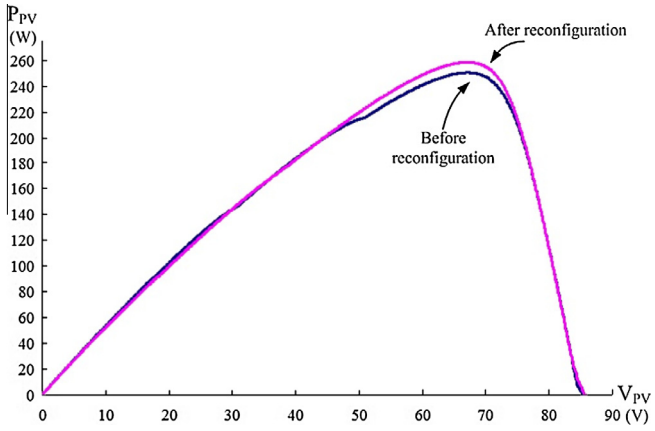

Fig. 13. Scenario 1: A comparison of the *P–V* characteristic curves before and after optimizing the configuration.

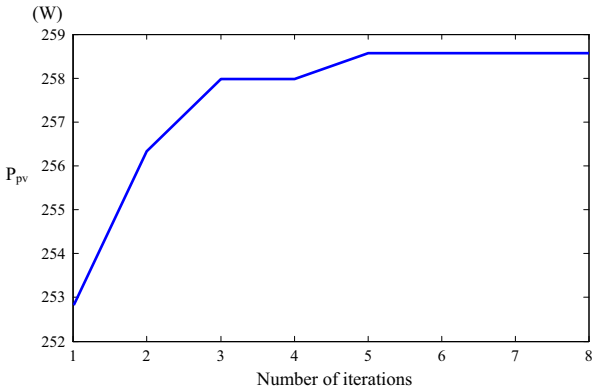

Fig. 14. Scenario 1: Changes in the g_{best} calculated using PSO.

optimal configuration controller sends control signals that enable or disable connections to achieve this connection scheme. By using this optimal configuration, the power output of the module array was enhanced, and the effects of shading or malfunctions were reduced.

5.2. MPPT of PV modules when shading or malfunctions occur

In PV power generation systems, if the PV module array is directly connected to the load, the power output of the array is determined by the power required by the load, and solar energy cannot be effectively or fully converted into power. Therefore, to ensure that the power output of the PV power generation system remains at the MPP in all operating conditions, an MPP tracker is used to connect the PV module array and the load to facilitate MPPT at all times. The commonly employed tracking methods include the voltage feedback method, constant voltage tracking method, power feedback method, perturb and observe method, and incremental conductance method [27]. However, when a PV module array experiences shading or malfunctions, the output characteristic curve may exhibit two or more peaks. Using current tracking methods, when a local MPP is found, the MPP tracker settles on the local peak and cannot track the actual MPP. Therefore, in this study, PSO was used to formulate the MPPT algorithm to eliminate the problem of tracking local MPPs, thereby increasing the overall power generated by the PV module array. The algorithm steps are described below [28].

Step 1. Initialize PSO parameters, and set the duty cycle of the boost converter as the particle location (X_j^k). Establish the objective function to be optimized ($P(V, I) = V_{PV} \times I_{PV}$). Here, the objective function value is the power output value of the PV module array.
Step 2. Output the particle duty cycle to the boost converter. Determine the voltage and current outputs of the PV module array, and calculate the power output of the module array. Here, the power output of the module array is the objective function value.
Step 3. Compare the observed current power output and p_{best} of each particle. If the current power output value is superior to p_{best}, update p_{best}. Compare p_{best} to g_{best}. If p_{best} is superior to g_{best}, then replace g_{best} with p_{best}.
Step 4. Using the PSO kernel equation, update the velocity and position of each particle.
Step 5. Repeat Steps 2–4 until the maximum iteration number is reached.
Step 6. Evaluate whether the shading or malfunction conditions have changed. If changes in the conditions are observed, return to Step 1. If not, remain at Step 6.

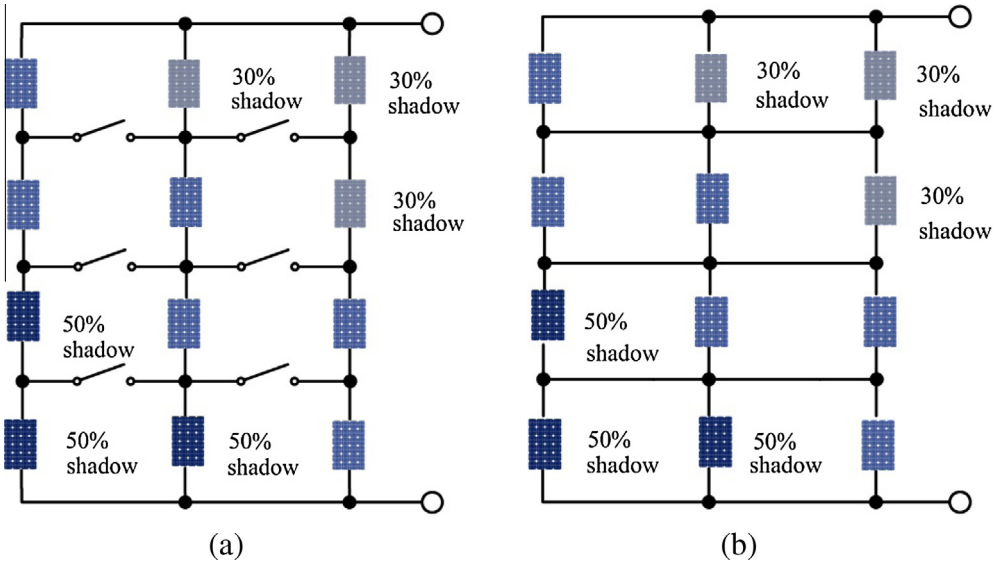

Fig. 15. Scenario 2: The connection scheme: (a) before; and (b) after reconfiguration.

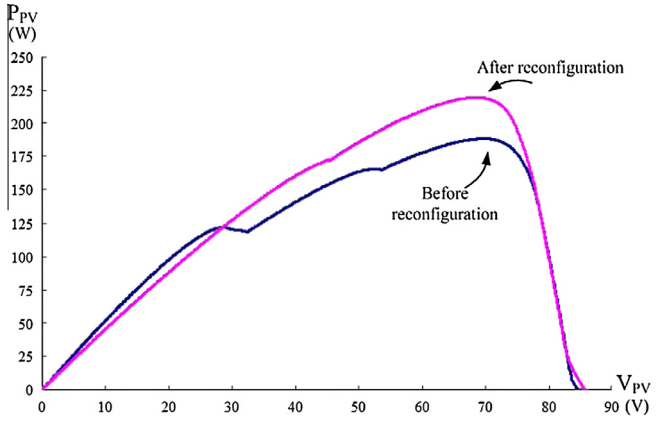

Fig. 16. Scenario 2: A comparison of *P–V* characteristic curves before and after optimizing the configuration.

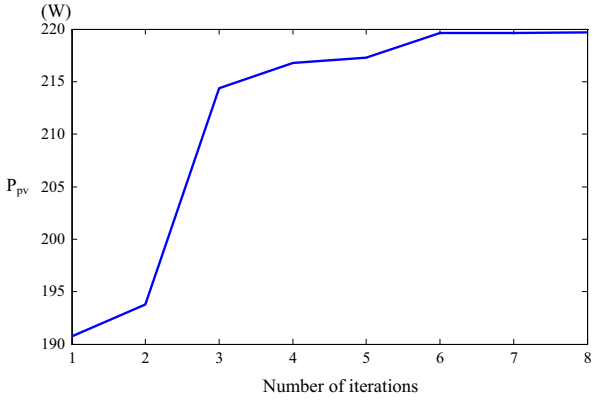

Fig. 17. Scenario 2: Changes in the g_{best} calculated using PSO.

5.3. Integrating MPPT and the optimal configuration of PV modules

To maximize the power generation and efficiency of PV module arrays, MPPT and a strategy for configuration optimization were adopted in this study. Current MPP readings in specific irradiation and module temperature conditions were compared with the MPP tracked by the MPP tracker. When a discrepancy between the MPPs confirmed the occurrence of partial shading or malfunctions, the optimal configuration strategy was activated. The algorithm steps are described below.

Step 1. Initialize PSO parameters and set the switch control signal as the particle location (X_j^k). Establish the objective function to be optimized ($P(V, I) = V_{PV} \times I_{PV}$). Here, the objective function value is the power output value of the PV module array.
Step 2. Output the particle control signal to the connection switch to enable or disable the connection. Wait for the MPP tracker to finish tracking.
Step 3. After tracking, determine the voltage and current outputs of the PV module array and calculate the power output of the module array. Here, the power output of the module array is the objective function value.
Step 4. Compare the observed current power output and p_{best} for each particle. If the current power output value is better than p_{best}, update p_{best}. Compare p_{best} to the g_{best}. If p_{best} is superior to g_{best}, update g_{best}.
Step 5. Using the PSO kernel equation, update the velocity and position of each particle.
Step 6. Repeat Steps 2–5 until the maximum iteration number is reached.
Step 7. Evaluate whether the shading or malfunction conditions have changed. If changes in the conditions are observed, return to Step 1. If not, remain at Step 7.

6. Experimental results

For the experiments performed in this study, Sanyo HIP-2717 modules were connected in 4-series/3-parallel arrays. Table 2 shows the electrical parameter specifications of the HIP-2717 module in STC [19]. Parameters relevant to the optimization algorithm used in this study are listed in Table 3. A PSoC microcontroller was used to implement the optimal configuration in various shading conditions.

In the first scenario, three modules in the upper left corner of the module array were 30% shaded, as shown in Fig. 12(a). Fig. 12(b) shows the connection scheme after optimizing the

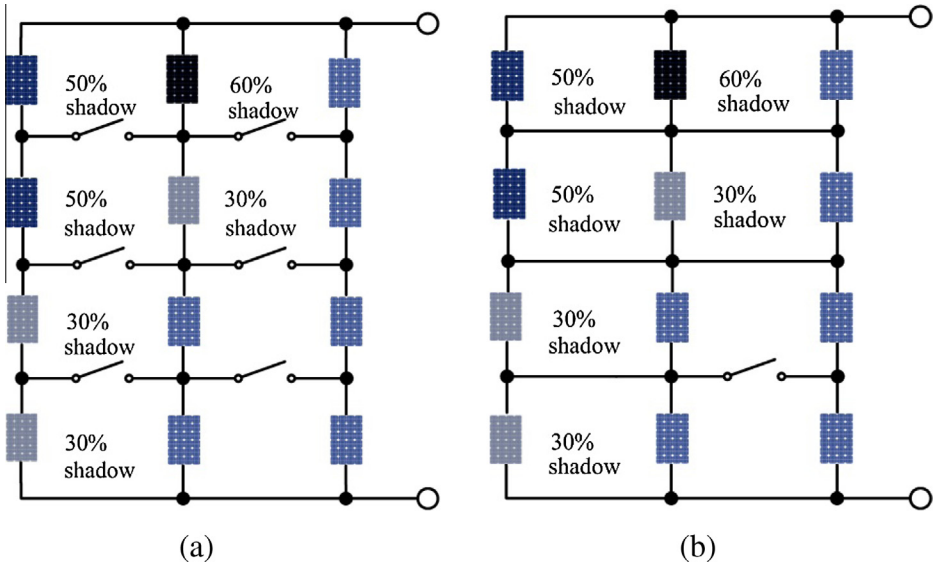

Fig. 18. Scenario 3: The connection scheme: (a) before; and (b) after reconfiguration.

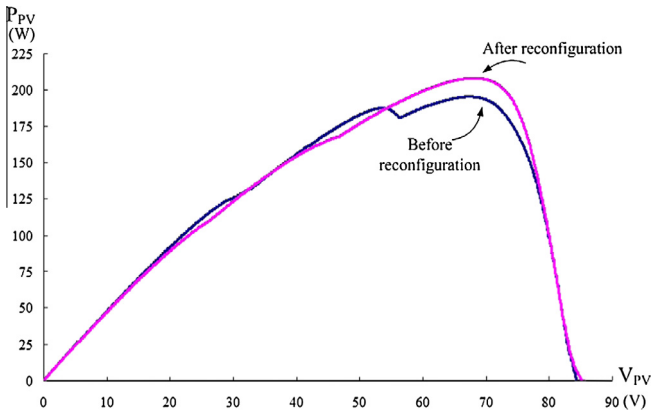

Fig. 19. Scenario 3: A comparison of *P–V* characteristic curves before and after optimizing the configuration.

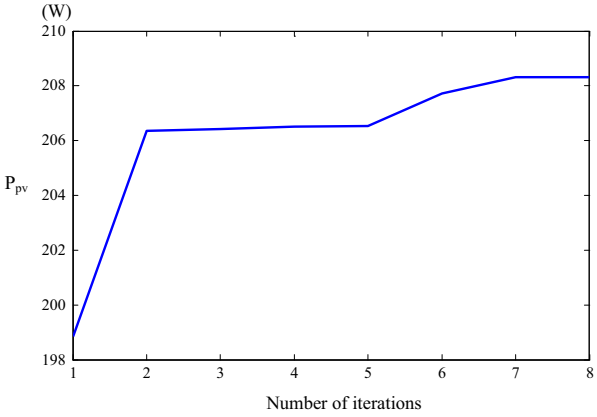

Fig. 20. Scenario 3: Changes in the g_{best} calculated using PSO.

configuration, and Fig. 13 shows the *P–V* characteristic curves before and after reconfiguration. The measured global best (g_{best}) calculation process using PSO is shown in Fig. 14. The maximum power output before and after reconfiguration are 250.51 W and 258.57 W, respectively. The results show that the maximum power output of the module array *P–V* characteristic curve after optimizing the configuration was 8.06 W (approximately 3.22%) higher than that before reconfiguration.

In the second scenario, three modules in the upper right corner of the module array were 30% shaded, and three modules in the lower left corner of the module array were 50% shaded. Fig. 15(a) and (b) shows the connection scheme before and after reconfiguration, respectively. Fig. 16 shows the *P–V* characteristic curves before and after reconfiguration. The measured global best (g_{best}) calculation process using PSO is shown in Fig. 17. The maximum power output before and after reconfiguration are 188.29 W and 219.70 W, respectively. The results show that the maximum power output of the module array *P–V* characteristic curve after optimizing the configuration was substantially increased by 31.41 W (approximately 16.68%) after reconfiguration.

In the third scenario, one module was 60% shaded, two modules were 50% shaded, and three modules were 30% shaded. Fig. 18(a) and (b) shows the connection scheme before and after reconfiguration, respectively. Fig. 19 shows the *P–V* characteristic curves before and after reconfiguration. The measured global best (g_{best}) calculation process using PSO is shown in Fig. 20. The maximum power output before and after reconfiguration are 195.74 W and 208.30 W, respectively. The results show that the maximum power output of the module array *P–V* characteristic curve after optimizing the configuration was substantially increased by 12.56 W (approximately 6.42%) after reconfiguration.

In the fourth scenario, a malfunction occurred in the second module in the second series. Fig. 21(a) shows the connection scheme before reconfiguration. Fig. 21(b) shows the connection scheme after optimizing the configuration, and Fig. 22 shows the *P–V* characteristic curves before and after reconfiguration. The measured global best (g_{best}) calculation process using PSO is shown in Fig. 23. The maximum power output before and after reconfiguration are 230.89 W and 240.40 W, respectively. The results show that even when a malfunction occurred, optimizing the configuration increased the maximum power output of the module array by 9.51 W (approximately 4.11%).

In the final scenario, malfunctions occurred in two modules in the first series. Fig. 24(a) shows the connection scheme before reconfiguration. Fig. 24(b) shows the connection scheme after optimizing the configuration, and Fig. 25 shows the *P–V* characteristic

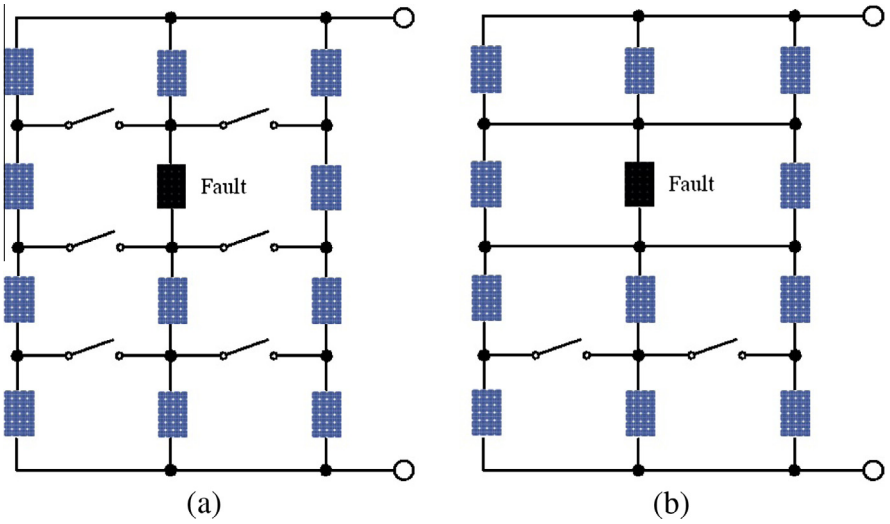

Fig. 21. Scenario 4: The connection scheme of an array with a malfunctioning module: (a) before; and (b) after reconfiguration.

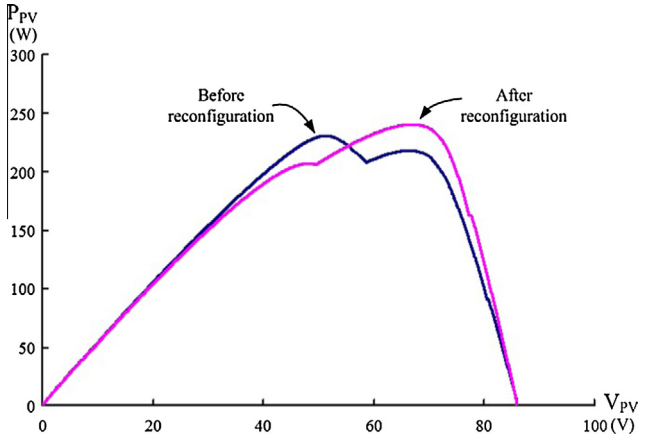

Fig. 22. Scenario 4: A comparison of *P–V* characteristic curves before and after optimizing the configuration.

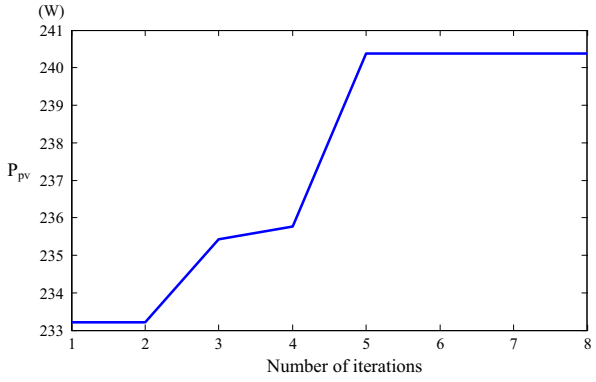

Fig. 23. Scenario 4: Changes in the g_{best} calculated using PSO.

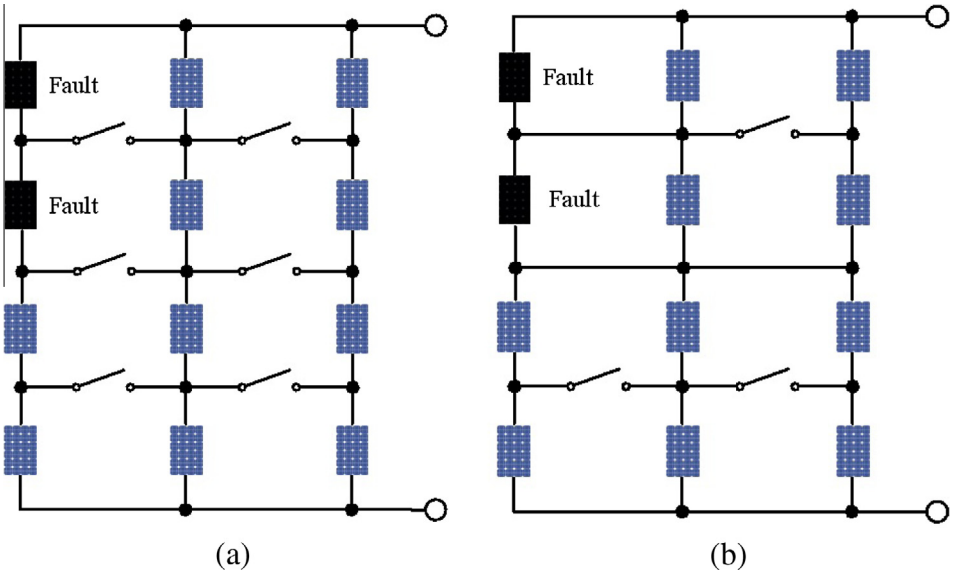

Fig. 24. Scenario 5: The connection scheme of an array with malfunctioning modules: (a) before; and (b) after reconfiguration.

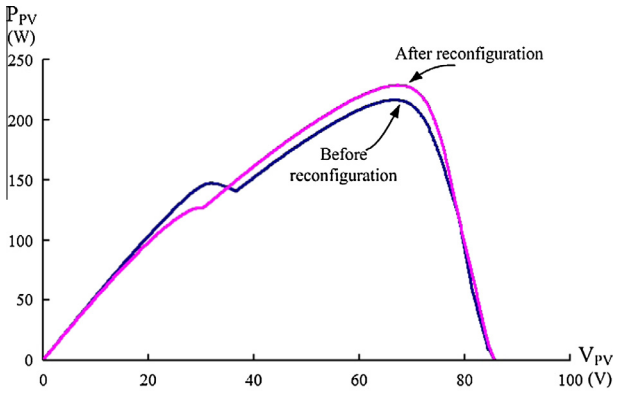

Fig. 25. Scenario 5: A comparison of *P–V* characteristic curves before and after optimizing the configuration.

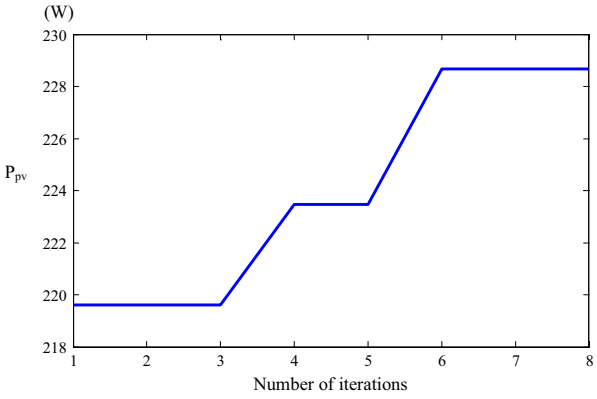

Fig. 26. Scenario 5: Changes in the g_{best} calculated using PSO.

curves before and after reconfiguration. The measured global best (g_{best}) calculation process using PSO is shown in Fig. 26. The maximum power output before and after reconfiguration are 216.56 W and 228.72 W, respectively. The results show that the maximum power output of the module array *P–V* characteristic curve after optimizing the configuration was substantially increased by 12.16 W (approximately 5.62%). Comparing to Scenario 4, the results show that greater numbers of malfunctioning modules increase the difference between the maximum power output before and after reconfiguration, as well as the ratio between the power output increase and the initial power output.

7. Conclusion

A PV module array with easily reconfigurable connection schemes was proposed in this study. When the module array experienced partial shading or malfunctions, PSO was performed to determine the optimal configuration for the module array. Because PSO is an algorithm developed based on the group foraging behavior of birds and uses distributed searches and memory, it causes all particles to exhibit a swarm effect and thus gradually approach the global best. This can reduce the effects that shading or malfunctions exert on PV module arrays. This study also explored the use of PSO in MPPT, employing the PSO characteristics relevant to MPPT to ensure that the PV module arrays operate at the actual MPP, thereby increasing the performance of PV power generation systems. Finally, PV module arrays in various shading and malfunction conditions were tested using experimental results, and the feasibility of the proposed strategy was verified.

Acknowledgment

The authors gratefully acknowledge the support of the National Science Council, Taiwan, Republic of China, under the Grant NSC 102-2221-E-167-009.

References

[1] Tang KH, Chao KH, Chao YW, Chen JP. Design and implementation of a simulator for photovoltaic modules. Int J Photoenergy 2012:1–6. Article ID 368931.
[2] Patel H, Agarwal V. Maximum power point tracking scheme for PV systems operating under partially shaded conditions. IEEE Trans Ind Electron 2008;55(4):1689–98.
[3] Gokmena N, Karatepea E, Silvestre S, Celik B, Ortega P. An efficient fault diagnosis method for PV systems based on operating voltage-window. Energy Convers Manage 2013;73:350–60.
[4] Tadj M, Benmouiza K, Cheknane A, Silvestre S. Improving the performance of PV systems by faults detection using GISTEL approach. Energy Convers Manage 2014;80:298–304.
[5] Silvestre S, Boronat A, Chouder A. Study of bypass diodes configuration on PV modules. Appl Energy 2009;86(3):1632–40.
[6] Diaz-Dorado E, Suarez-Garcia A, Carrillo C, Cidras J. Influence of the shadows in photovoltaic systems with different configurations of bypass diodes. In: International symposium on power electronics, electrical drives, automation and motion; 2010. p. 134–9.
[7] Nguyen TL, Low KS. A global maximum power point tracking scheme employing direct search algorithm for photovoltaic systems. IEEE Trans Ind Electron 2010;57(10):3456–67.
[8] Koutroulis E, Blaabjerg F. A new technique for tracking the global maximum power point of PV arrays operating under partial-shading conditions. IEEE J Photovoltaics 2012;2(2):184–90.
[9] Sera D, Teodorescu R, Hantschel J, Knoll M. Optimized maximum power point tracker for fast-changing environmental conditions. IEEE Trans Ind Electron 2008;55(7):2629–37.
[10] Solorzano J, Egido MA. Automatic fault diagnosis in PV systems with distributed MPPT. Energy Convers Manage 2013;76:925–34.
[11] Mozaffari Niapour SAKH, Danyali S, Sharifian MBB, Feyzi MR. Brushless DC motor drives supplied by PV power system based on Z-source inverter and FL-IC MPPT controller. Energy Convers Manage 2011;52:3043–59.
[12] Akkaya R, Kulaksız AA, Aydog˘du O. DSP implementation of a PV system with GA-MLP-NN based MPPT controller supplying BLDC motor drive. Energy Convers Manage 2007;48:210–8.
[13] Tsang KM, Chan WL. Model based rapid maximum power point tracking for photovoltaic systems. Energy Convers Manage 2013;70:83–9.
[14] Altin N, Ozdemir S. Three-phase three-level grid interactive inverter with fuzzy logic based maximum power point tracking controller. Energy Convers Manage 2013;69:22–6.
[15] Tsang KM, Chan WL. Three-level grid-connected photovoltaic inverter with maximum power point tracking. Energy Convers Manage 2013;65:221–7.
[16] Nguyen D, Lehman B. An adaptive solar photovoltaic array using model-based reconfiguration algorithm. IEEE Trans Ind Electron 2008;55(7):2644–54.
[17] Shams El-Dein MZ, Kazerani M, Salama MMA. Novel configurations for photovoltaic farms to reduce partial shading losses. In: IEEE power and energy society general meeting; 2011. p. 1–5.
[18] Alahmad M, Chaaban MA, Lau SK, Shi J, Neal J. An adaptive utility interactive photovoltaic system based on a flexible switch matrix to optimize performance in real-time. Solar Energy 2012;86(3):951–63.
[19] SANYO photovoltaic module HIP-230HDE1 specifications. <http://www.glea.pt/downloads/painel_fotovoltaico_sanyo_220w.pdf>.
[20] Ramaprabha R, Mathur BL. A comprehensive review and analysis of solar photovoltaic array configurations under partial shaded conditions. Int J Photoenergy 2012:1–16. Article ID 120214.
[21] Wang YJ, Hsu PC. An investigation on partial shading of PV modules with different connection configurations of PV cells. Energy 2011;36:3069–78.
[22] Eberhart RC, Kennedy J. A new optimizer using particle swarm theory. In: Proceedings of sixth international symposium on micro machine and human science, Nagoya Japan; 1995.
[23] Kennedy J, Eberhart RC. Particle swarm optimization. In: Proceedings of IEEE international conference on neural networks, Piscataway NJ; 1995.
[24] Liu Y, Niu B. A novel PSO model based on simulating human social communication behavior. Int J Photoenergy 2012:1–21. Article ID 791373.
[25] Liu A, Zahara E, Yang MT. A modified NM-PSO method for parameter estimation problems of models. Int J Photoenergy 2012:1–12. Article ID 530139.
[26] Ishaque K, Salam Z, Amjad M, Mekhilef S. An improved particle swarm optimization (PSO)-based MPPT for PV with reduced steady-state oscillation. IEEE Trans Power Electron 2012;27(8):3627–38.
[27] Chao KH, Lee YH. A maximum power point tracker with automatic step size tuning scheme for photovoltaic systems. Int J Photoenergy 2012:1–10. Article ID 176341.
[28] Liu YH, Huang SC, Huang JW, Liang WC. A particle swarm optimization-based maximum power point tracking algorithm for PV systems operating under partially shaded conditions. IEEE Trans Energy Convers 2012;27(4):1027–35.